

## DETECTION OF [Si vi] 1.962 MICRONS AND NEW OBSERVATIONS OF INFRARED H, [Fe ii], AND H<sub>2</sub> LINE EMISSION IN THE SEYFERT GALAXY NGC 1068<sup>1</sup>

E. OLIVA

Osservatorio Astrofisico di Arcetri

AND

A. F. M. MOORWOOD

European Southern Observatory

Received 1989 June 19; accepted 1989 October 2

### ABSTRACT

We present measurements of several infrared lines in NGC 1068 including the [Si vi] transition at 1.962  $\mu\text{m}$  which is detected for the first time in an extragalactic object. This line is among the brightest IR features ( $\sim 5$  times stronger than H<sub>2</sub> 2.121  $\mu\text{m}$ ), is broad ( $\Delta v \sim 1100 \text{ km s}^{-1}$ ), and has a profile similar to He I 1.083  $\mu\text{m}$ . The possibility of using the [Si vi] line to trace Seyfert activity and the origin of the H, [Fe ii], and H<sub>2</sub> lines are briefly discussed.

*Subject headings:* galaxies: individual (NGC 1068) — galaxies: nuclei — galaxies: Seyfert — infrared: spectra

### I. INTRODUCTION

Spectra of only a few active galactic nuclei have so far been obtained in the infrared at  $\lambda > 1 \mu\text{m}$ . Those Seyfert nuclei observed are found to exhibit strong He I 1.083  $\mu\text{m}$ , Paschen and Brackett series H recombination lines and, in the case of Seyfert 1's, O I 1.129  $\mu\text{m}$ . Some galaxies containing active nuclei also show [Fe ii] and H<sub>2</sub> line emission whose origin is presently unclear but which is generally believed to arise in circumnuclear gas which is shock-excited by supernova remnants resulting from star-forming activity and/or mass outflows or possibly other interactions with the active nucleus (see Moorwood 1989 for a review).

NGC 1068 is one of the brightest and best studied active galactic nuclei. Although exhibiting the prototype Seyfert 2 optical spectrum, this galaxy appears to also contain a broad-line-emitting region more characteristic of Seyfert 1's but which is visually obscured along the line of sight and detectable only in polarized reflected light (Antonucci and Miller 1985). Star formation is also occurring over the central few kpc (e.g., Telesco *et al.* 1984). This was also the first extragalactic object in which infrared lines of H<sub>2</sub> were detected (Thompson, Lebofsky, and Rieke 1978) and infrared spectra covering variously the He I, H, [Fe ii], and H<sub>2</sub> lines have subsequently been obtained by various observers (e.g., Hall *et al.* 1981; Ward 1988; Kawara, Nishida, and Gregory 1987; Kawara, Nishida, and Taniguchi 1988; Kawara, Nishida, and Phillips 1989).

More recently we have obtained spectra of NGC 1068 at resolving power  $R \sim 1500$  in various parts of the 1–5  $\mu\text{m}$  region primarily to investigate further the origin of the [Fe ii] and H<sub>2</sub> lines and also to search for lines from highly ionized species which are not expected to be associated with normal OB stars (i.e., in classical starburst models) but which require the hard UV photons generated by the central engine in standard Seyfert models or by extreme W-R-type stars in starburst model proposed by Terlevich and Melnick (1985). In the visible, such lines from highly ionized species, e.g., [Fe vii] 6087 Å and [Fe x] 6375 Å are relatively common in Seyfert

nuclei (e.g., Veilleux 1988 and references therein). Many forbidden transitions of coronal species also fall in the infrared but have so far only been observed in two novae (Grasdalen and Joyce 1976; Greenhouse *et al.* 1988) and in two high-excitation planetary nebulae (Ashley and Hyland 1988).

The main purpose of this *Letter* is to present and discuss the first detection of one of these coronal lines, [Si vi] at 1.962  $\mu\text{m}$ . We also comment briefly on the origin of the H, [Fe ii], and H<sub>2</sub> lines in the light of our new results.

### II. OBSERVATIONS

The data were collected in 1988 October using the ESO grating-array spectrometer IRSPEC (Moorwood *et al.* 1986) mounted on the ESO 3.6 m telescope. The nucleus of the galaxy was optically centered inside the 6"  $\times$  6" instrumental aperture using a slit-viewing TV; centering was maintained by autoguiding on an offset star. To eliminate sky emission and instrumental offsets, the galaxy and the reference position 30" south were alternatively measured by moving a focal plane wobbling mirror after each detector read-out (5 s at  $\lambda < 3 \mu\text{m}$ ); beam switching was used only at  $\lambda > 3 \mu\text{m}$ . Each section of the spectrum was "double-sampled" by merging two measurements at grating angles corresponding to a wavelength shift of half a pixel in order to properly sample the instrumental profile. Total integration time was 20 minutes per each double-sampled section of the spectrum. The region around [Si vi] 1.962 was measured twice on different nights. To correct the spectra for atmospheric absorption features two nearby stars of very different spectral types, namely BS 779 (B2 IV) and BS 509 (G8 V), were observed immediately before and/or after NGC 1068. This procedure gave a good cancellation of the atmospheric features even around 1.96  $\mu\text{m}$  and made it possible to correct for the features intrinsic to the reference stars by assuming that they had no lines in common. Additional, single-sampled spectra around the [Fe ii] 1.644  $\mu\text{m}$  and H<sub>2</sub> 2.121  $\mu\text{m}$  lines were also obtained using a narrower 2" wide slit at several positions separated by 2" along the NS line through the nucleus. The seeing during these measurements was better than 1". The data have been reduced using MIDAS, the standard ESO software package. For each 32 pixel exposure, the

<sup>1</sup> Based on observations collected at the European Southern Observatory, La Silla, Chile.

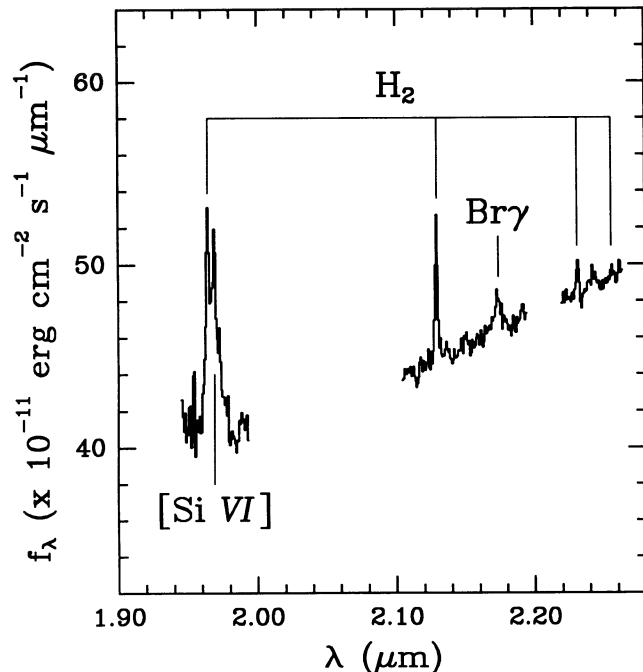


FIG. 1a

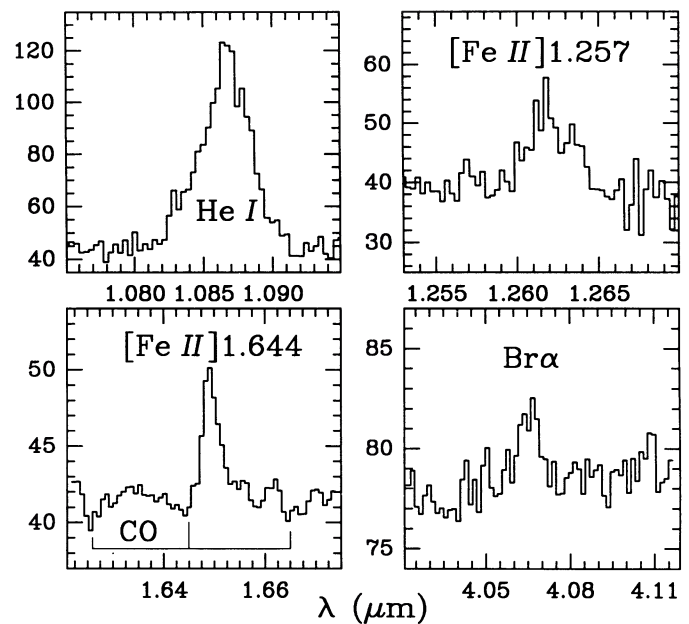


FIG. 1b

FIG. 1.—(a) Flux-calibrated spectrum of NGC 1068 showing the prominent and broad line of [Si VI] at  $\lambda_{\text{rest}} = 1.962 \mu\text{m}$ . The  $\text{H}_2$  lines are (left to right) (1, 0)S(3), (1, 0)S(1), (1, 0)S(0), and (2, 1)S(1) (not detected). (b) Flux-calibrated spectra of NGC 1068 around He I 1.083  $\mu\text{m}$ , [Fe II] 1.257  $\mu\text{m}$ , [Fe II] 1.644  $\mu\text{m}$ , and Br $\alpha$  4.051  $\mu\text{m}$ . Flux scale is in units of  $10^{-11} \text{ ergs cm}^{-2} \text{ s}^{-1} \mu\text{m}^{-1}$ .

raw spectra of NGC 1068 and of BS 779 (cleaned of intrinsic features) were ratioed. The various sections were then merged together allowing for small continuum fluctuations among the different exposures ( $< 5\%$  in all cases) and flux-calibrated assuming  $f_{\lambda}(\text{BS 779}) = 5.0 \times 10^{-9} (\lambda/2.2 \mu\text{m})^{-3.7} \text{ ergs cm}^{-2} \text{ s}^{-1} \mu\text{m}^{-1}$ .

### III. RESULTS

A mosaic of the measured spectral sections is displayed in Figures 1a and 1b. The [Si VI] line is clearly visible at  $\sim 1.97 \mu\text{m}$ , blended with  $\text{H}_2$  (1, 0)S(3) (the narrow peak at  $\lambda_{\text{rest}} = 1.957$ ). The best-fit central wavelength of the [Si VI] line is  $\lambda_{\text{rest}} = 1.9615 \pm 0.0014$ , in good agreement with the value found by Ashley and Hyland (1988;  $\lambda = 1.9613 \pm 0.002$ ) which is the best determination so far available. The [Si VI] line is quite broad, and its amplitude is  $\sim 20\%$  of the continuum level. Both facts make the detection quite safe as an incorrect atmospheric cancellation should produce large pixel-to-pixel variations and cannot account for smooth and prominent features. All the measured line fluxes and widths are listed in Table 1. Our fluxes for Br $\gamma$  and the  $\text{H}_2$  lines at  $\lambda > 2 \mu\text{m}$  are similar to those measured by Hall *et al.* (1981) while the Br $\gamma$  line appears slightly, though not significantly, narrower. Normalized line profiles are displayed in Figure 2. The profile of the [Si VI] line is similar to that of He I 1.083 which is the broadest among the observed lines. The apparent asymmetry of [Fe II] 1.644, which is not observed in the [Fe II] 1.257 line, is most probably produced by CO second-overtone band absorption at  $\lambda_{\text{rest}} = 1.64 \mu\text{m}$  in the underlying continuum (in confirmation other CO features are also visible at  $\lambda_{\text{rest}} = 1.62, 1.66$ ; cf. Fig. 1b). The spatial scans across the nucleus with a  $2''$  slit shown in Figure 3 reveal that both the [Fe II] and  $\text{H}_2$  emission extends over  $\sim 4''$  (200 pc). Whereas the  $\text{H}_2$  lines are

narrow ( $\leq 300 \text{ km s}^{-1}$ ) on all the measured positions, however, the [Fe II] line is broad ( $\approx 800 \text{ km s}^{-1}$ ) on the nucleus but narrow (unresolved at  $300 \text{ km s}^{-1}$ ) on the position 2''S. The hydrogen lines Br $\gamma$  and Br $\alpha$  have similar widths. No broader component of Br $\alpha$  is visible to a limit of  $\sim 1\%$  of the continuum level within the spectral interval covered by our spectrum ( $\approx 7000 \text{ km s}^{-1}$ ).

### IV. DISCUSSION

#### a) The [Si VI] 1.962 Micron Line

The [Si VI] line at  $1.962 \mu\text{m}$  ( $2p^5 \ ^2P_{1/2} \rightarrow 2p^5 \ ^2P_{3/2}$ ) is the only forbidden line expected from  $\text{Si}^{+5}$ . This transition has a relatively large probability ( $A = 2.38 \text{ s}^{-1}$ ; Mendoza 1983) and, therefore, a high critical density ( $n_c \sim 10^8 \text{ cm}^{-3}$ ) which might

TABLE 1  
OBSERVED LINE PARAMETERS

Transition	Flux <sup>a</sup>	$\Delta v^b$
He I 1.083 .....	320 (30)	1100 (190)
[Fe II] 1.257 .....	39 (4)	800 (150)
[Fe II] 1.644 .....	30 (2)	800 (300)
$\text{H}_2(1, 0)S(3)$ 1.957 .....	15 (4)	300 (220)
[Si VI] 1.962 .....	75 (15)	1100 (220)
$\text{H}_2(1, 0)S(1)$ 2.121 .....	15 (1)	300 (200)
Br $\gamma$ 2.166 .....	13 (2)	900 (190)
$\text{H}_2(1, 0)S(0)$ 2.223 .....	4.4 (0.7)	300 (190)
$\text{H}_2(2, 1)S(1)$ 2.247 .....	$< 2.1$	...
Br $\alpha$ 4.051 .....	38 (7)	800 (220)

<sup>a</sup> Observed line intensity in units of  $10^{-14} \text{ ergs cm}^{-2} \text{ s}^{-1}$ . Uncertainties are in parentheses.

<sup>b</sup> Full width half-maximum of the line in  $\text{km s}^{-1}$ . Numbers in parentheses are the instrumental resolution.

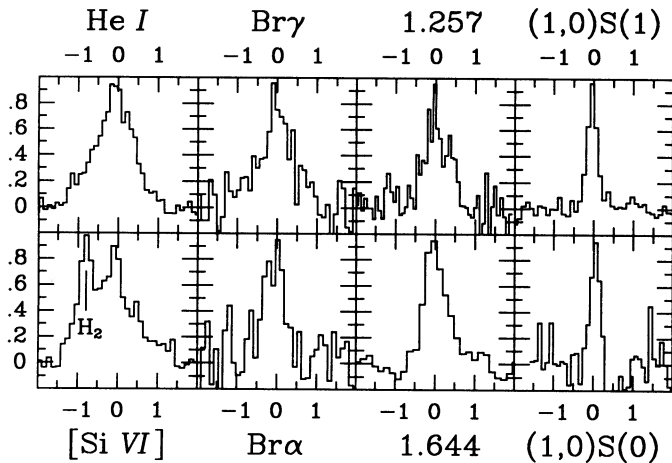


FIG. 2.—Normalized line profiles plotted as a function of velocity ( $v = 0$  corresponds to the redshift of NGC 1068). The velocity scale is in units of  $1000 \text{ km s}^{-1}$ ; negative velocities are for blueshifts.

account for the larger width of this line, compared to  $[\text{Fe II}]$ , and its similarity with the profile of  $\text{He I}$  if part of the emission comes from high-density, high-velocity regions. The observed ratio  $[\text{Si VI}]/\text{Br}\gamma = 5.8$  is very similar to that found in the planetary nebula NGC 6302 ( $[\text{Si VI}]/\text{Br}\gamma = 5.9$ ; Ashley and Hyland 1988) and is remarkably close to the value recently computed by Korista and Ferland (1989;  $[\text{Si VI}]/\text{Br}\gamma = 6.0$ ) in a model where both the coronal and the hydrogen lines are produced in a low-density medium photoionized by a Seyfert nucleus. It seems reasonable therefore to assume that in NGC 1068 the  $[\text{Si VI}]$  line and a significant fraction of  $\text{Br}\gamma$  are produced by gas photoionized by the Seyfert nucleus. Shock excitation,

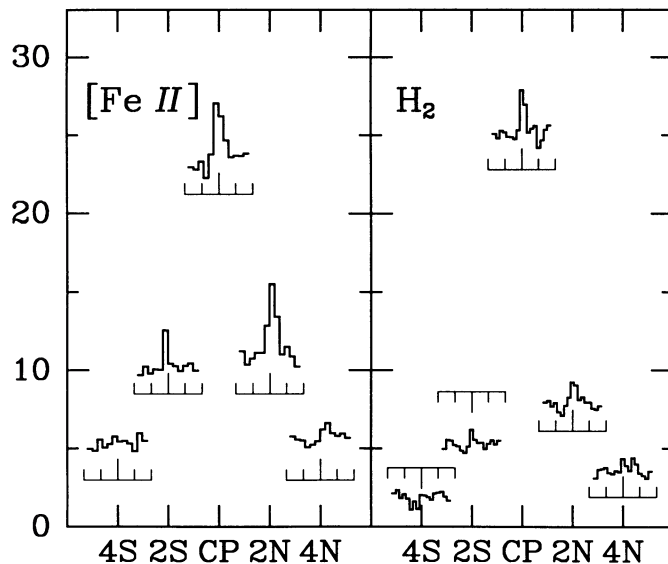


FIG. 3.—North-south scans of  $[\text{Fe II}]$   $1.644 \mu\text{m}$  and  $\text{H}_2$   $2.121 \mu\text{m}$  taken through a  $6'' \times 2''$  ( $\alpha \times \delta$ ) slit. Flux scale is in units of  $10^{-11} \text{ ergs cm}^{-2} \text{ s}^{-1} \mu\text{m}^{-1}$ . The single-sampled spectra (cf. § II) are shown on a velocity scale with each tick mark corresponding to  $1000 \text{ km s}^{-1}$ . For  $[\text{Fe II}]$  each pixel corresponds to  $300 \text{ km s}^{-1}$ , and the line is clearly resolved on the central and  $2''\text{N}$  positions while narrower  $2''\text{S}$ . For  $\text{H}_2$ , each pixel corresponds to  $200 \text{ km s}^{-1}$  and the appearance of the line being on two pixels is characteristic of its being centered between two pixels, in which case the true width is likely to be less than  $300 \text{ km s}^{-1}$ .

although not *a priori* excluded, appears unlikely on the basis of a spectrum of the supernova remnant RCW 103 where the  $[\text{Si VI}]$  line is not detected to a limit of 5% of  $[\text{Fe II}]$   $1.644 \mu\text{m}$  (Oliva, Moorwood, and Danziger 1989b).

For future work we note that the ionization potential of  $\text{Si VI}$  is  $167 \text{ eV}$ , an energy in between that necessary to produce  $\text{Fe VII}$  ( $100 \text{ eV}$ ) and  $\text{Fe X}$  ( $235 \text{ eV}$ ). It is therefore not unreasonable to expect that galaxies exhibiting relatively strong  $[\text{Fe VII}]$   $6087 \text{ \AA}$  and  $[\text{Fe X}]$   $6375 \text{ \AA}$  lines could also contain a considerable amount of  $\text{Si VI}$ . Compared to other active galaxies NGC 1068 has somewhat weak  $[\text{Fe X}]$  lines ( $[\text{Fe X}]/[\text{Fe VII}] \sim 0.1$ ; e.g. Veilleux 1988) and already exhibits a prominent  $[\text{Si VI}]$   $1.962 \mu\text{m}$  line. It is therefore promising to search for the  $[\text{Si VI}]$  transition in high-excitation galaxy nuclei, especially in those with redshifts large enough to move the line into the cleanest part of the  $K$  window (i.e.,  $0.05 < z < 0.2$ ).

### b) Origin of Other Infrared Lines

As extinction decreases with increasing wavelength, one of the interests in observations of the infrared hydrogen recombination lines is the possibility of detecting visually obscured broad-line regions in Seyfert 2 nuclei. In NGC 1068 a broad-line region is known to exist from visible spectropolarimetric observations as noted already in the Introduction. The fact that we find comparable widths for the  $\text{Br}\alpha$  and  $\text{Br}\gamma$  lines and an intensity ratio of  $2.9 \pm 0.7$  which is consistent with the standard recombination theory and relatively little reddening implies, however, that the extinction to this region is still high enough to obscure it even at  $\approx 4 \mu\text{m}$ . This supports the same conclusion drawn previously by DePoy (1987) and does not confirm the much larger width ( $1700 \text{ km s}^{-1}$ ) and  $\text{Br}\alpha/\text{Br}\gamma$  ratio ( $\approx 12$ ) claimed by Kawara, Nishida, and Gregory (1987), and Kawara, Nishida, and Phillips (1989) on the basis of a  $\text{Br}\alpha$  spectrum covering  $\sim 2200 \text{ km s}^{-1}$  around the line center.

With regard to the origin of the  $[\text{Fe II}]$  and  $\text{H}_2$  line emission we have previously argued on the basis of a survey of 35 galaxy nuclei ranging from pure  $\text{H II}$  region-like to Seyfert 1 that both species are most probably produced in circumnuclear gas which is shock excited by supernova remnants resulting from star-forming activity with, in the case of composite starburst/Seyfert nuclei, some extra contribution from mechanical interactions with the active nucleus (Moorwood and Oliva 1988). The ratios of  $[\text{Fe II}]$  and  $\text{H}_2$  to  $\text{Br}\gamma$  measured in NGC 1068 are comparable to those measured in other composite nuclei in our survey sample and about 2 and 4 times larger, respectively, than typically observed in pure starburst nuclei. These results and the much larger widths measured for the  $[\text{Fe II}]$  compared with the  $\text{H}_2$  lines are similar to those obtained in a somewhat larger aperture by Kawara, Nishida, and Taniguchi (1988) who also concluded that these lines are probably shock excited by an AGN wind. It should be noted that, whereas the  $\text{Br}\gamma$  in starburst nuclei arises in gas photoionized by stars, both Seyfert-ionized gas and  $\text{H II}$  regions contribute in composite nuclei. In NGC 1068, in particular, it is likely that the  $\text{Br}\gamma$  emission is dominated by the active nucleus. If the excitation of all three lines in this case is dominated by the active nucleus, therefore the fact that the line ratios are only of the order of a factor of 2 higher than in starburst nuclei implies that the ratio of mechanical energy to ionizing radiation in an active nucleus must be very comparable to that in a starburst. An alternative possibility discussed recently in detail is that the  $\text{H}_2$  emission in active nuclei might result from X-ray heating of a molecular torus  $\sim 1 \text{ pc}$  in size surrounding the nucleus (Krolik and Lepp

1989). Although obscuration of the active nucleus in NGC 1068 is attributed to the presence of such a torus, however, the much larger spatial extent of the H<sub>2</sub> emission ( $\approx 200$  pc) argues against it being the dominant contributor in this case. The higher spatial resolution scans across the nucleus shown in Figure 3 were also made with a view to measuring the relative spatial extent of the [Fe II] and H<sub>2</sub> emission following the discovery of a spatial shift between the line emission peaks in NGC 4945 (Moorwood and Oliva 1989). At the lower S/N ratio achieved in NGC 1068, however, it is difficult to conclude more than that the FWHM is similar ( $\approx 4''$ ) for both. If anything, however, the H<sub>2</sub> emission is slightly more peaked on the nucleus than the [Fe II] which also appears to be shifted to the N. These results are therefore difficult to reconcile with the proposal of Kawara, Nishida, and Taniguchi (1988) that the relative narrowness of the H<sub>2</sub> lines could be accounted for if they arise in molecular material lying outside the [Fe II]-

emitting region. Our observations also fail to confirm the significant extinction to the [Fe II]-emitting region which, although difficult to reconcile with the symmetry of the [O III] 5007 Å line, was invoked by Kawara *et al.* to account for the asymmetry of the [Fe II] 1.644 line. As discussed above, this apparent asymmetry is in fact due to CO absorption in the underlying stellar continuum. It is not present in the [Fe II] 1.257 line which arises from the same upper level and the observed intensity ratio [Fe II] 1.257/1.644 =  $1.3 \pm 0.16$  is consistent with the intrinsic, unreddened ratio (cf. Oliva, Moorwood, and Danziger 1989a). Although more extensive studies are clearly required, therefore, we conclude that the available data are more consistent with a model in which the [Fe II] and H<sub>2</sub>-emitting clouds occupy similar volumes and the differences in linewidths result from collisional dissociation of H<sub>2</sub> in the higher velocity clouds.

## REFERENCES

- Antonucci, R. R. J., and Miller, J. S. 1985, *Ap. J.*, **297**, 621.  
 Ashley, M. C. B., and Hyland, A. R. 1988, *Ap. J.*, **331**, 532.  
 DePoy, D. L. 1987, in *Infrared Astronomy with Arrays, Proc. Workshop on Ground-based Astronomical Observations with Infrared Array Detectors*, ed. C. G. Wynn-Williams and E. E. Becklin (Honolulu: Institute for Astronomy, University of Hawaii), p. 246.  
 Grasdalen, G. L., and Joyce, R. R. 1976, *Nature*, **259**, 187.  
 Greenhouse, M. A., Grasdalen, G. L., Hayward, T. L., Gehrz, R. D., and Jones, T. J. 1988, *A.J.*, **95**, 172.  
 Hall, D. N. B., Kleinmann, S. G., Scoville, N. Z., and Ridgway, S. T. 1981, *Ap. J.*, **248**, 898.  
 Kawara, K., Nishida, M., and Gregory, B. 1987, *Ap. J. (Letters)*, **321**, L35.  
 Kawara, K., Nishida, M., and Phillips, M. M. 1989, *Ap. J.*, **337**, 230.  
 Kawara, K., Nishida, M., and Taniguchi, Y. 1988, *Ap. J. (Letters)*, **328**, L41.  
 Korista, K. T., and Ferland, G. J. 1989, *Ap. J.*, **343**, 678.  
 Krolik, J. H., and Lepp, S. 1989, preprint.  
 Mendoza, C. 1983, in *IAU Symposium 103, Planetary Nebulae*, ed. D. R. Flower (Dordrecht: Reidel), p. 143.  
 Moorwood, A. F. M. 1989, in *Infrared Spectroscopy in Astronomy*, ed. A. C. H. Glasse, M. F. Kessler, and R. Gonzales-Riesta (ESA SP290), in press.  
 Moorwood, A. F. M., Biereichel, P., Finger, G., Lizon, J. L., Meyer, M., Nees, W., and Paureau, J. 1986, *Messenger*, **44**, 19.  
 Moorwood, A. F. M., and Oliva, E. 1988, *Astr. Ap.*, **203**, 278.  
 ———. 1989, in *IAU Symposium 134, Active Galactic Nuclei*, ed. D. E. Osterbrock and J. S. Miller (Dordrecht: Kluwer), in press.  
 Oliva, E., Moorwood, A. F. M., and Danziger, I. J. 1989a, *Astr. Ap.*, **214**, 307.  
 ———. 1989b, in *Infrared Spectroscopy in Astronomy*, ed. A. C. H. Glasse, M. F. Kessler, and R. Gonzales-Riesta (ESA SP 290), in press.  
 Telesco, C. M., Becklin, E. E., Wynn-Williams, C. G., and Harper, D. A. 1984, *Ap. J.*, **282**, 427.  
 Terlevich, R., and Melnick, J. 1985, *M.N.R.A.S.*, **213**, 841.  
 Thompson, R. I., Lebofsky, M. J., and Rieke, G. H. 1978, *Ap. J. (Letters)*, **222**, L49.  
 Veilleux, S. 1988, *A.J.*, **95**, 1695.  
 Ward, M. 1988, *Adv. Space Res.*, Vol. 8, No. 2-3, p. 39.

A. F. M. MOORWOOD: ESO, European Southern Observatory, Karl Schwarzschild Str. 2, D8046, Garching bei München, Federal Republic of Germany

E. OLIVA: Osservatorio Astrofisico di Arcetri, Largo E. Fermi 5, I-50125, Firenze, Italy